ELSEVIER

Journal of Biomechanics 32 (1999) 255–266

JOURNAL OF BIOMECHANICS

# Magnitudes of local stress and strain along bony surfaces predict the course and type of fracture healing

L.E. Claes*, C.A. Heigele

*Department Unfallchirurgische Forschung und Biomechanik, University of Ulm, Helmholtzstraße 14, 89081 Ulm, Germany*

Received in final form 1 September 1998

**Abstract**

A new quantitative tissue differentiation theory which relates the local tissue formation in a fracture gap to the local stress and strain is presented. Our hypothesis proposes that the amounts of strain and hydrostatic pressure along existing calcified surfaces in the fracture callus determine the differentiation of the callus tissue. The study compares the local strains and stresses in the callus as calculated from a finite element model with histological findings from an animal fracture model. The hypothesis predicts intramembranous bone formation for strains smaller approximately $\pm$ 5% and hydrostatic pressures smaller than $\pm$ 0.15 MPa. Endochondral ossification is associated with compressive pressures larger than about $-$ 0.15 MPa and strains smaller than $\pm$ 15%. All other conditions seemed to lead to connective tissue or fibrous cartilage. The hypothesis enables a better understanding of the complex tissue differentiation seen in histological images and the mechanical conditions for healing delayed healing or nonunions. 

*Keywords:* Bone healing; Mechanical stimuli; Tissue differentiation

## 1. Introduction

Flexible fixation of long bone fractures results in the formation of periosteal callus. The biomechanical function of the callus is the reduction of the initial movement to such an extent that the bone fragments can unite with bony bridges. This is achieved by enlarging the cross-sectional area of the bridging tissue and its mechanical stiffness. The osteogenic potential, influenced by blood supply, hormones, or growth factors (Brand and Rubin, 1987; Hulth, 1989) and the biomechanical conditions at the fracture site (Brand and Rubin, 1987; Hulth, 1989; Kenwright et al., 1986; Rhinelander, 1979) are the two most important factors guiding the healing process. Given a sufficient vascularity, the course of fracture healing seems to be mainly influenced by the interfragmentary movement determined by the applied load and the stability of the fixation (Claes et al., 1995a; Goodship and Kenwright, 1985; Kenwright and Goodship, 1989; Perren, 1974; Schenk, 1986). However, the amount of interfragmentary movement that would optimize the healing process and avoid failures is still not known.

Following a fracture, hematoma occurs which develops a granulation tissue (Frost, 1989; Willenegger et al., 1971). Typically the new bone formation in this "soft callus" starts at the periosteal and endosteal surface of the cortical bone at some distance from the fracture (Einhorn, 1995). This bone formation proceeds in the direction of the fracture gap (Ashhurst 1986; Brighton, 1984; McKibbin, 1978; Sevitt, 1981; Fig. 1). Intramembranous bone formation can be observed adjacent to zones of endochondral ossification (Fig. 6c). In the late stage of callus healing only a small gap of nonossified tissue separates the callus wedges. It contains a variety of tissue types including fibrocartilage, cartilage, granulation tissue, intramembranous bone and calcifying cartilage (Figs. 1b,c, and 6c).

Pauwels (1960) developed a theory for the tissue differentiation in response to the local mechanical stresses. He hypothesized that deviatoric stresses, which are always accompanied by strain in some direction, are a specific stimulus for the formation of fibrous connective tissue or bone. Hydrostatic stresses on the other hand are responsible for the formation of cartilaginous tissue.

*Corresponding author. Tel.: + 49 731 5023481; fax: + 49 731 5023498; e-mail: claes@sirius.medizin.uni-ulm.de

0021-9290/99/$ – see front matter 
PII: S0021-9290(98)00153-5

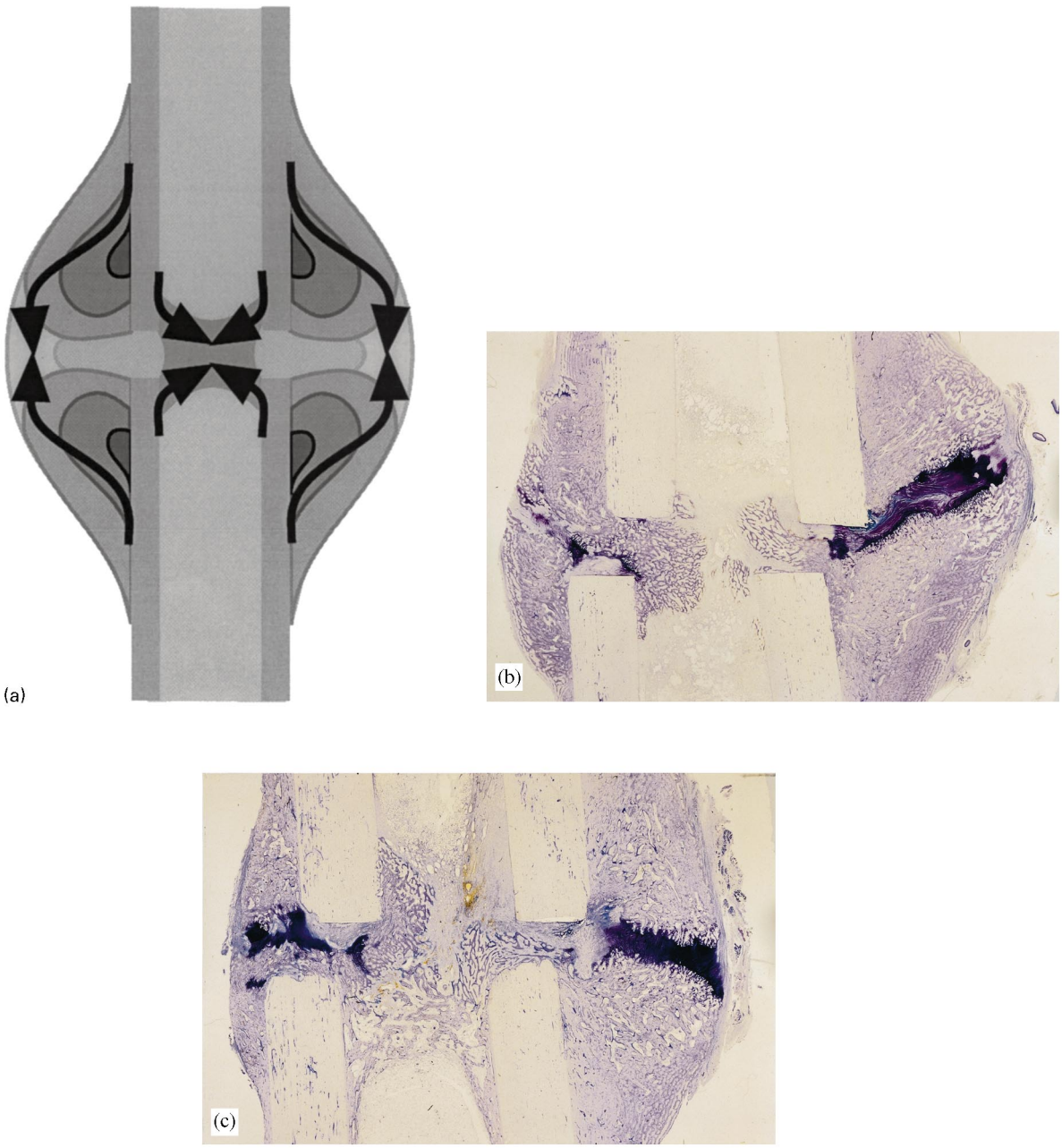


Fig. 1. (a) Schematical drawing of callus formation under flexible fixation of a fracture. The arrows indicate the direction of bone apposition. (b, c) Longitudinal histological sections of callus formation nine weeks p.o. in two sheep metatarsal. Zones of fibrocartilage (violet) remain in the middle of the periosteal callus. Bone healing occurs in this zone by endochondral ossification. In the most peripheral part of the periosteal callus and in the endosteal area, callus formation occurs by intramembranous bone formation. The osteotomy gap still remains fibrous tissue and does not show a complete bony bridging.

The knowledge of the stresses and strains on cells in a fracture callus tissue and their influence on cell differentiation would lead to a better understanding of the mechanically controlled tissue differentiation process and could help to improve fracture treatment. However, it is not possible to determine the stresses and strains of the cells in a fracture callus in vivo. To estimate the local tissue strains and stresses in a fracture callus we employed the finite element method (FEM).

Several research groups (Ament et al, 1994; Beaupre et al., 1992; Biegler and Hart, 1992; Blenman et al., 1989; Carter et al., 1988; Cheal et al., 1991; DiGioia et al., 1986, 1995) have analysed the local mechanical situation in the fracture callus or in the fracture gap by the finite element

method. Carter et al. (1988) developed a new tissue differentiation theory, which correlated new tissue formation with the local stress histories. The tissue differentiation theories of Carter et al. Blenman et al. Beaupre et al. only qualitatively and not quantitatively described the relationship between the ossification pattern and the loading history. All research groups used the strain energy density or the stress invariants, like dilatational stress or deviatoric stress to quantify the local mechanical stimuli. They did not investigate the actual local deformation, in terms of local strain or stress components and did not predict the type of tissue formation resulting from these mechanical signals.

Our hypothesis proposes that new bone formation in fracture healing occurs primarily along fronts of existing bone or calcified tissue and that the type of bone healing (intramembranous or endochondral) depends on the local strain and stress magnitudes. The following study tests this hypothesis by comparing the calculated local strains and stresses in callus tissue based on a FEM study with histological findings from an in vivo study (Claes et al., 1995a).

## 2. Materials and methods

### 2.1. Animal model

The effect of interfragmentary movement on fracture healing was investigated in an animal experiment on sheep. The sheep underwent a standardized transverse osteotomy of the right metatarsal. The osteotomy was stabilized by a specially designed external ring fixator (Claes et al., 1995a) which provided extremely high bending and torsional stiffness while allowing axial movements through a telescoping system. Weight bearing in the operated limb produced an axial telescoping corresponding to a controlled interfragmentary movement. Maximum axial movement was controlled by an adjustment nut set to a given depth. The change of interfragmentary movement by callus formation was monitored weekly by a displacement transducer placed between the distal and proximal fixator frame. The signal was transmitted telemetrically to a personal computer (Claes et al., 1995a). The study was approved according to relevant laws and regulations by the government review board (Regierungspräsidium Tübingen, No. 407). The finite element models were based on a group of seven sheep with 3 mm gap size and 1 mm interfragmentary movement. For the labeling of newly formed bone, calcein green was injected 4 weeks post operative (p.o.) and reverin 8 weeks p.o. All animals were killed at 9 weeks p.o. Undecalcified bone histology was prepared with paragon surface staining. Using fluorescence microscopy the polychrome sequential bone labelling was documented and analysed. The results were presented elsewhere (Augat et al., 1994a,b; Claes et al., 1995a, 1997).

### 2.2. Finite element model

Three two-dimensional axisymmetric finite element (FE) models were generated using ANSYS version 5.2 (CAD-FEM, Munich, Germany). Each model represents one specific healing stage. The first model reflects the morphology occurring one week after fracture. The second and third model describe the fourth and eighth healing week, respectively. The basic overall geometry of the cortex and the callus region is identical for all three models. Tissue differentiation and gradual stiffening of the callus tissue are the fundamental processes of secondary fracture healing. These processes were simulated by changing the element material properties from one stage to the next. The characterization of the histomorphological sequence of the healing process and the types of tissue involved were based on the previously described animal study (Claes et al., 1995a). Based upon the histologic sections we assumed that these three geometries represent typical ossification patterns (Fig. 4).

Fig. 2a shows the geometrical dimensions of one-quarter of the finite element model of the callus. We assumed a rotational symmetry along the long bone axis ($y$) and mirror-image symmetry through the plane of the osteotomy ($x$) and, therefore modelled only one-quarter of the total geometry. Seven distinct regions were modelled (Fig. 2b). Axisymmetric 8-node elements were used. Approximately 5000 elements were utilized in each healing stage, the number of nodes was about 15 000 (Fig. 3). For verifying the finite element study and testing the convergence, we performed three additional finite element studies and varied the number of elements (5000 or 9000 elements) and the element type (four-node or eight-node element). We evaluated the strain and hydrostatic pressure in the elements which are located directly under the cortical fragments and show the highest strain and hydrostatic pressure values. There were only small differences in the strain and pressure values between the 9500 eight-node study and the 5000 eight-node study.

To describe progressive stiffening of the callus, we assumed five tissue types differing in their elastic material properties (Table 1). The tissue material properties were obtained from indentation tests on tissue sections from different callus regions (Augat et al., 1996) and were similar to values taken by others (Biegler and Hart, 1992; Davy and Connolly, 1982).

In the initial healing stage, the callus consisted only of connective tissue (Fig. 4a). The second model contained callus of intermediate stiffness in a small region along the periosteum, and soft callus tissue adjacent to it, while the remainder consisted of initial connective tissue (Fig. 4b, about 4 weeks p.o.). In the third model the callus tissue contained five tissue types: initial connective tissue, soft callus, intermediate stiffness callus, stiff callus and chondroid ossification zone (Fig. 4c). Isotropic material behaviour was assumed for all tissue types.

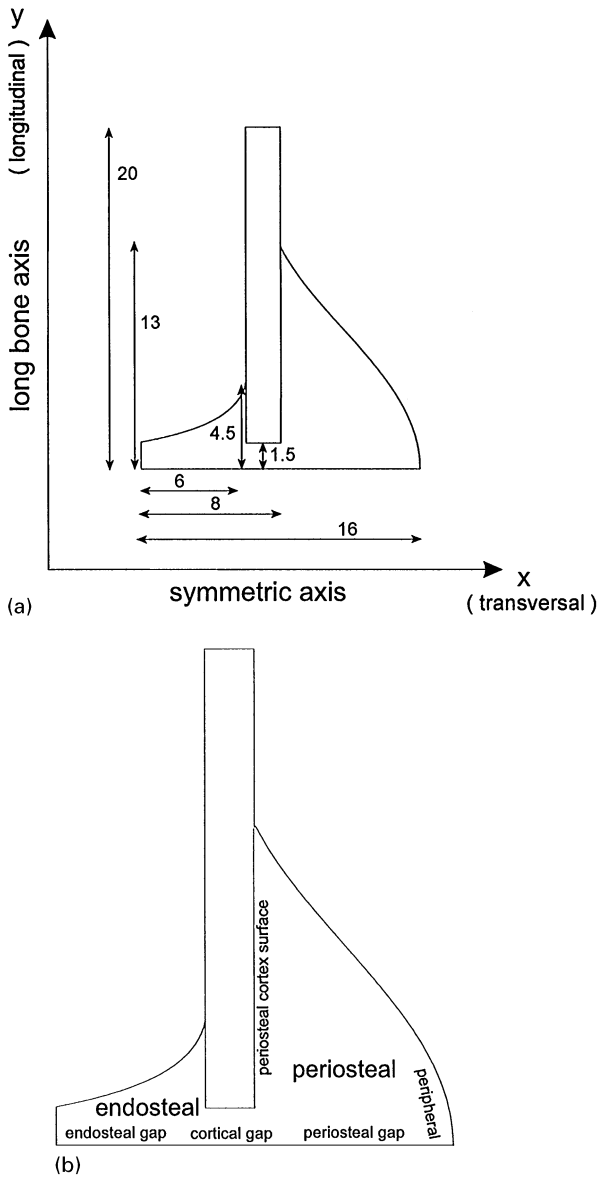


Fig. 2. (a) Geometrical dimensions of one quarter of the FE-model of the callus region. (b) Identification of the different callus regions.

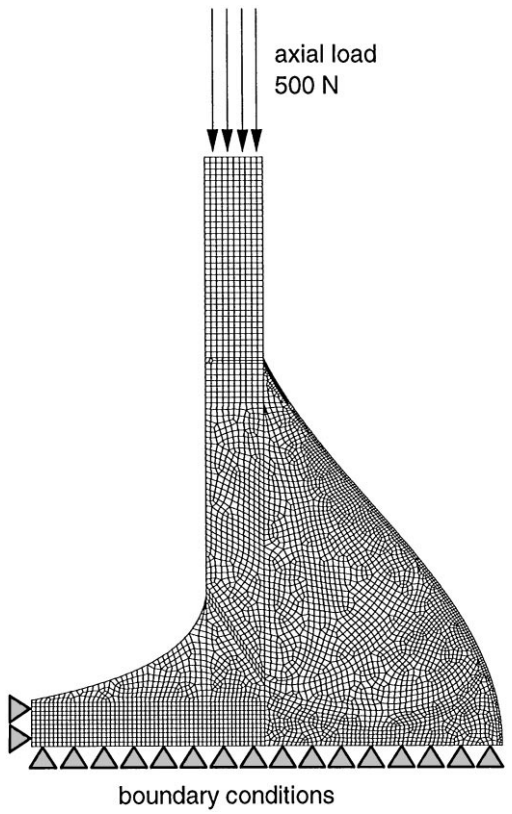


Fig. 3. Finite element model: mesh, loading and boundary conditions (quarter model).

Table 1
Material properties of the different tissue types involved in the fracture healing process

| Tissue type | | Young's modulus (MPa) | Poisson ratio | Mooney–Rivlin constants |
|---|---|---|---|---|
| Initial connective tissue | ICT | 3 | 0.4 | 0.293<br>0.177 |
| Soft callus | SOC | 1000 | 0.3 | — |
| Intermediate stiffness callus | MSC | 3000 | 0.3 | — |
| Stiff callus | SC | 6000 | 0.3 | — |
| Chondroid ossification zone | COZ | 10 000 | 0.3 | — |
| Cortex | C | 20 000 | 0.3 | — |
| Fascie | F | 250 | 0.4 | — |

Initially a fracture callus exhibits a rubberlike behaviour when tested mechanically: it has low strength, low stiffness, and large elongation (Brighton, 1984). Therefore, to describe the initial connective tissue we used the nonlinear hyperelastic Mooney–Rivlin Potential (ANSYS User's Manual, vol. IV). For all other tissue types, we idealized the tissue behaviour by material linearity (Hooke's Law).

Sussman and Bathe (1987) introduced a displacement–pressure ($u/p$) finite element formulation for the nonlinear analysis of compressible and almost incompressible solids. In this special formulation the displacements and hydrostatic pressure, normally computed from the displacement field, are calculated by separate interpolations (ANSYS User's Manual, vol. III). The $u/p$ formulation starts with a modified potential that explicitly includes the pressure variables:

$$W + Q = W - \frac{1}{2k}(p - \bar{p})^2,$$

where $W$ is the original potential, here the Mooney–Rivlin potential, $Q$ the energy augmentation due to

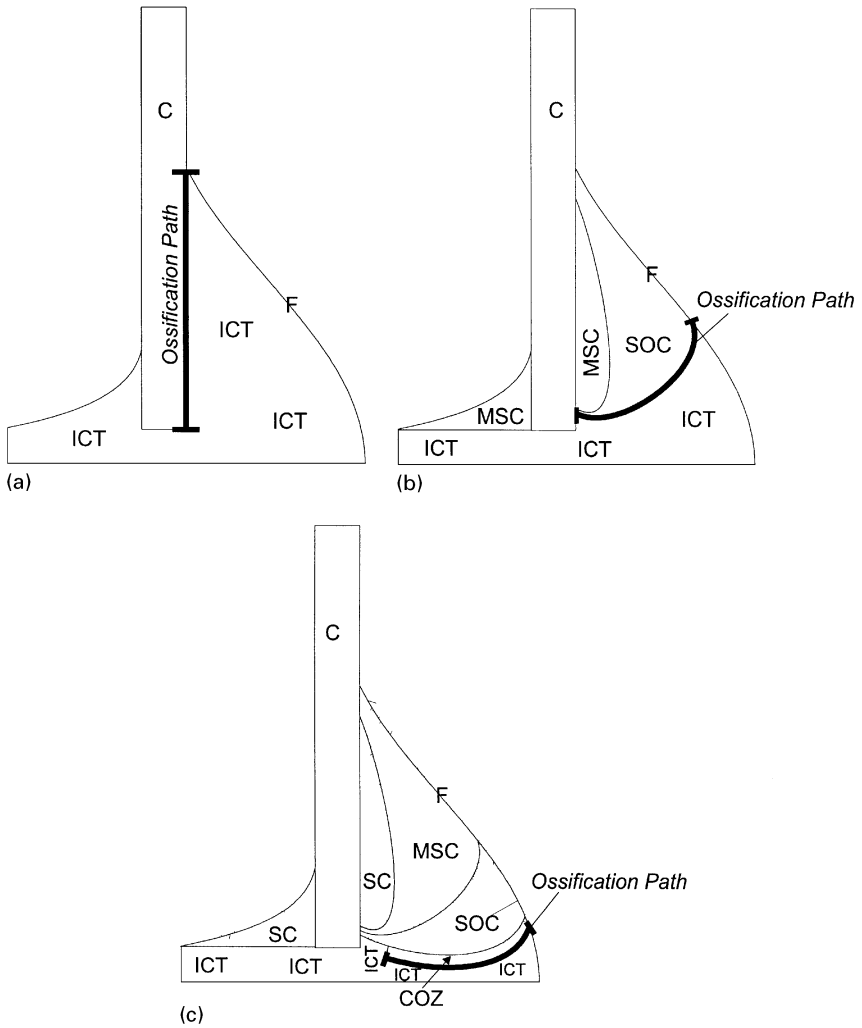


Fig. 4. Material properties and ossification paths for the three modelled healing stages (for description of the various abbreviations see Table 1): (a) first stage ( ~ 1 week p.o.); (b) second stage ( ~ 4 weeks p.o.); (c) third stage ( ~ 8 weeks p.o.).

volume constraint condition, $k$ the bulk modulus, $p$ the pressure obtainable from $W$ alone, $\bar{p}$ the separately interpolated pressure (hydrostatic pressure).

The $u/p$ finite formulation was only employed for calculating the stresses and strains in the initial connective tissue.

The metatarsals of the sheep were loaded with an axial force of approximately 500 N as shown by gait analysis and analytical calculations (Duda et al., 1998). Accordingly, in our models the cortex was loaded with an axial force of 500 N (Fig. 3). The boundary conditions were as follows: the displacement degree of freedom (DOF) of the nodes on the $x$-axis in the $y$-direction were set to zero; the displacement DOF in the $x$-direction of the nodes on the $y$-axis were restricted (gray arrows in Fig. 3).

For the first verification of our results, we compared the temporal decrease of the interfragmentary movement in the in vivo animal study with the results of our FE study. Then we determined the global strain field and the global hydrostatic pressure distribution for all three

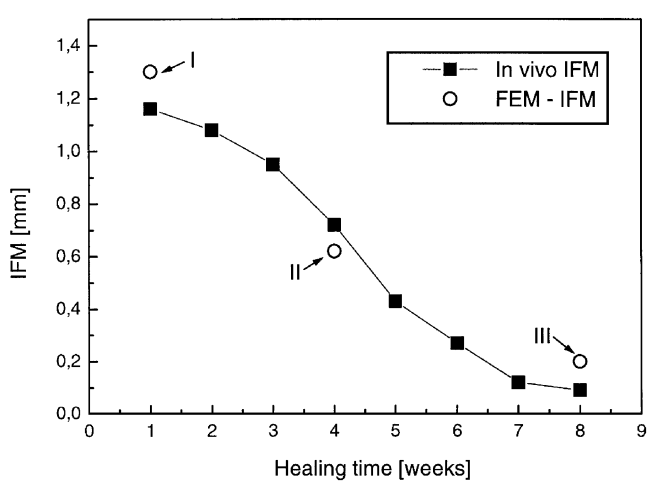


Fig. 5. Course of interfragmentary movement (IFM) versus healing time of an osteotomy of a sheep metatarsus with 3 mm osteotomy gap and 1.2 mm initial IFM compared with the calculated IFM by the FE-model.

healing stages. For each healing stage we calculated the local strain components and the hydrostatic pressure along the ossification paths (Fig. 4). The calculated results were compared with the histological sections of callus specimens from the in vivo study (Claes et al., 1995a). The endosteal regions were not analysed because the endosteal bone formation appears to be guided by biological factors rather than mechanical factor (Einhorn, 1993; McKibbin, 1978).

## 3. Results

### 3.1. Animal experiment

The interfragmentary movement (IFM) decreased with increasing healing time by increasing callus cross section and callus stiffness (Claes et al., 1995a). Fig. 5 shows a typical curve for a sheep with a gap size of 3 mm and an IFM of 1.2 mm. After 1 week the IFM was 1.16 mm and after 8 weeks the IFM reached values below 0.1 mm

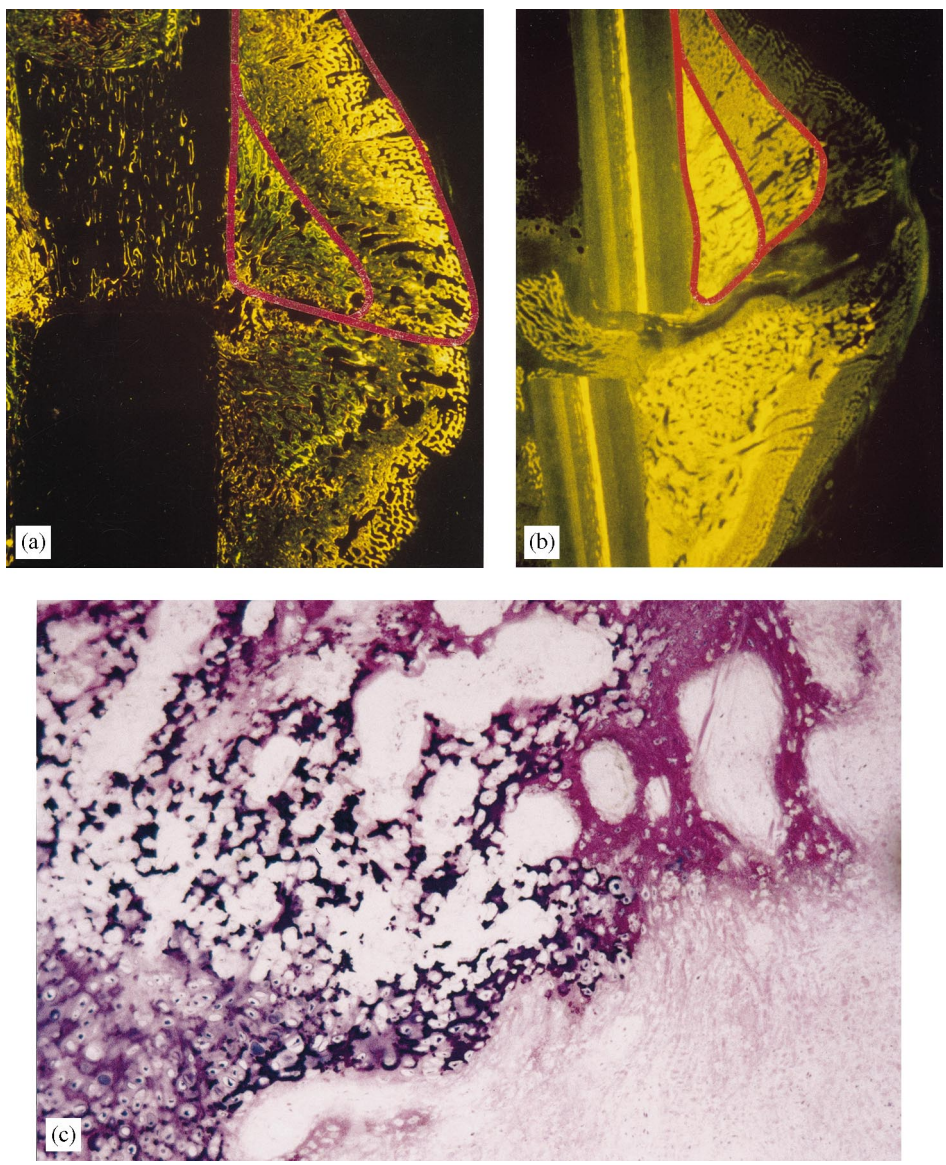


Fig. 6. Longitudinal section through the lateral callus of sheep metatarsal after osteotomy and external fixation, 9 weeks postoperatively. (a) (b) Fluorescence light microscopy of the callus of two individual sheep demonstrating two phases of callus formation; (green: calcein green (4 weeks); yellow: reverin (8 weeks)). Red lines indicating the border line of bone formation at 4 and 8 weeks corresponding to the analysed path lines of the FEM study. The callus in the left picture shows already bony bridging whereas in the right picture a fracture line is still visible. (c) Higher magnification of a remaining fracture gap with both types of bone healing; intramembranous bone formation (at the right) and endochondral ossification (in the centre), (paragon staining, magnification 75 times).

which is in the range of the precission of the measurement system (Claes et al., 1995a).

The paragon stained sections (Figs. 1b, 1c, and 6c) showed a remaining gap filled with connective tissue and fibrous cartilage at the level of the osteotomy. The fluorescence images (Fig. 6a,b) showed the sequence of new bone formation in the callus with green labelling at 4 weeks (calcein green) and yellow labelling at 8 weeks (reverin). Bone formation increases in diameter towards the osteotomy gap (Fig. 6a,b).

At 9 weeks both types of bone healing, intramembranous bone formation and endochondral ossification (Fig. 6c) occur simultaneously, but at characteristic locations. Intramembranous bone formation leads first to bridging of the fracture gap at the periphery, while endochondral ossification replaces the remaining fibrocartilage in the central region progressively and finally closes the fracture gap in the periosteal callus area (Figs. 1b,c, 6a,b,).

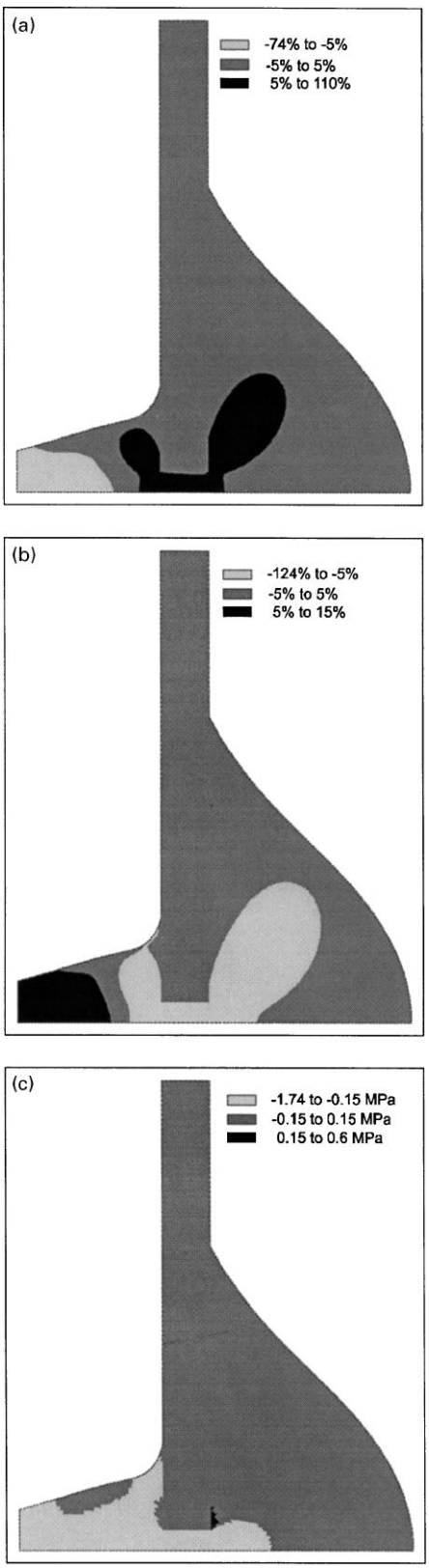


### 3.2. Finite element model

Good agreement between the amount of reduction of IFM in the in vivo study and the FE-study (Fig. 5) was observed. In the FE-study, we calculated an IFM of 1.3 mm for the first healing stage (in vivo 1.16 mm), an IFM of 0.62 mm for the second stage (in vivo 0.72 mm) and an IFM of 0.62 mm of 0.2 mm for the last healing stage (in vivo 0.09 mm).

The comparison of the histological tissue distribution and calculated strain and hydrostatic pressure fields led us to investigate the following characteristic areas.

Areas of low ( $< \pm 5\%$) and high ( $> \pm 5\%$) transverse ($x$) and longitudinal ($y$) strain:

In the first healing stage all areas along the periosteal and endosteal surface (Fig. 7a and b: dark gray regions) showed low strains. Around the cortical edges (Fig. 10a: path 0–1) and the cortical gap we found large strains (Fig. 7a and b).

In the second healing stage low strain was calculated in the bony callus and at the peripheral surface of the newly formed bone (Fig. 8a and b: dark grey regions, Fig. 10b: path 5.6–6.6). Similar conditions were found for a small area near the periosteum (Fig. 10b: path 0–0.2) and for the endosteum (Fig. 8a and b). Higher strains were computed for the cortical gap and at the periosteal callus front (Fig. 8a and b).

In the third healing stage low strains were found in the most peripheral part of the periosteal callus (Fig. 9a and b: dark grey regions, Fig. 10c: path 6.6–6.8) and in the

Fig. 7. First healing stage: global distribution of strain and hydrostatic pressure fields: (a) strain in $x$-direction (%), (negative strain means a reduction, positive strain means an increase in $x$-direction); (b) strain in $y$-direction (%), (negative strain means a reduction, positive strain means an increase in $y$-direction); (c) hydrostatic pressure (MPa), (negative hydrostatic pressure means a reduction of the volume, positive pressure means an expansion of the volume).

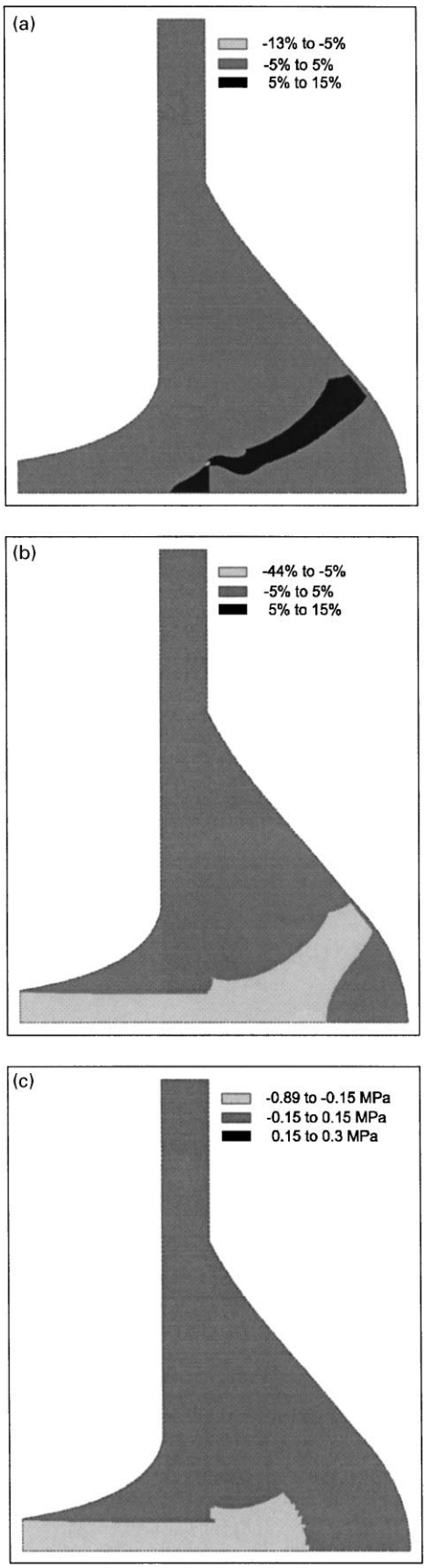


Fig. 8. Second healing stage: global distribution of strain and hydrostatic pressure fields. (a) strain in $x$-direction (%). (b) strain in $y$-direction (%). (c) hydrostatic pressure (MPa).

whole endosteal region. Strains were relatively high ($> 10\%$, Fig. 9b: light grey regions, Fig. 10c) in longitudinal direction at the centre of the remaining periosteal callus surface.

Areas of low ($< \pm 0.15$ MPa) and high ($> \pm 15$ MPa) hydrostatic pressure:

In the first healing stage the major part of the periosteal callus volume and whole periosteal surface showed low pressures (Fig. 7c, Fig. 10a, path 1–9.6). Higher pressures were observed endosteally near the cortical gap and around the cortical edges next to the cortical gap. In the second healing stage low hydrostatic pressure was calculated for the peripheral part of the periosteal callus (Fig. 8c, Fig. 10b, path 3–6.6) whereas high pressure values occurred in the remaining soft tissue gap. The third healing stage showed similar conditions with low pressures at the periphery of the periosteal callus (Fig. 9c, Fig. 10c, path 5–6.8) and high pressure at the remaining soft tissue gap. Another small region of low pressure was found next to the cortical edge at the periosteum (Fig. 9c).

The comparison of typical locations of intramembranous bone formation and endochondral ossifications with the calculated strain and hydrostatic pressure allowed us to describe the following mechanical conditions for the various types of bone healing.

Region A (Fig. 11) with a surface strain $< \pm 5\%$, a hydrostatic pressure $< \pm 0.15$ MPa, and intramembranous bone formation. These conditions were calculated at the following locations: In the first healing stage at the periosteum in some distance from the osteotomy gap (from path value 1 to the end of the path, Fig. 10a); in the second and in the third healing stage at the peripheral part of the periosteal callus (from 5.6 to 6.6, Fig. 10b and from 6.6 to 6.8, Fig. 10c) and at the periosteal edge of the cortical gap (from 0 to 0.2, Fig. 10b).

Region B with surface $< \pm 15\%$, negative hydrostatic pressure values greater than $-0.15$ MPa (Fig. 11), and endochondral ossification (Fig. 6b): The first healing stage showed no regions with these specific mechanical conditions. In the second healing stage these conditions were found between path value 0.2 and path value 2.8 (Fig. 10b) and in the third stage from the beginning of the path to path value 4.9 (Fig. 10c). For all other mechanical conditions connective tissue or fibrous cartilage was found in the histological section. Fibrous cartilage was mainly seen in areas with high compressive hydrostatic pressures larger than $-0.15$ MPa.

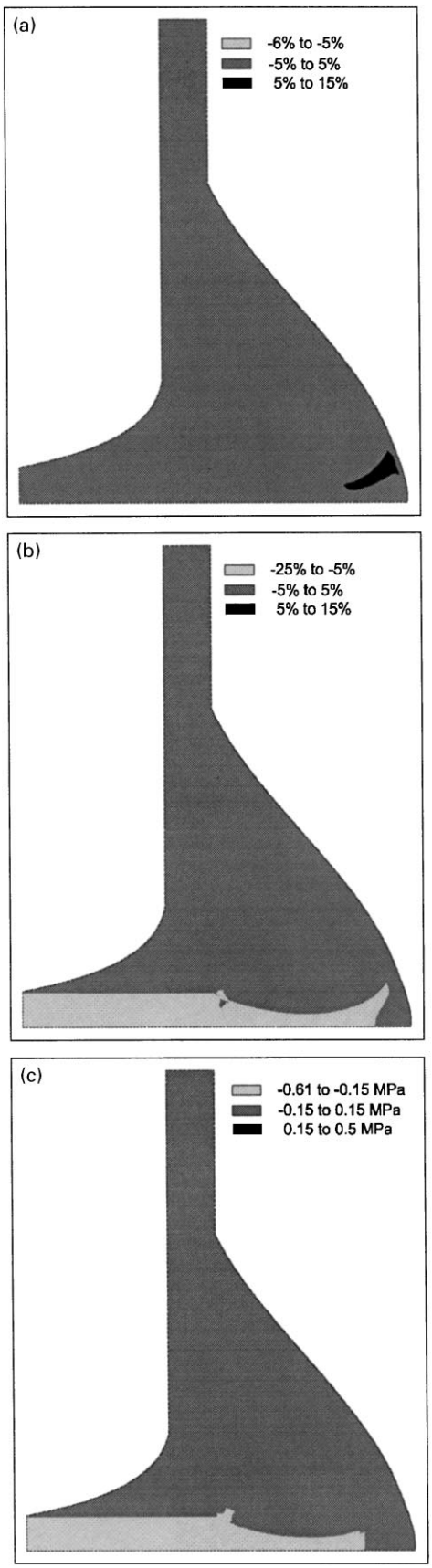


## 4. Discussion

Our hypothesis that the amount of strain and hydrostatic pressure along the calcified surface in the callus are the determinant factors for the differentiation of the callus tissue was supported by the results of this FE study. The comparison of the local strains and hydrostatic pressures along the ossification paths with typical histological images, allowed us to attribute intramembranous bone formations, endochondral ossification as well as the occurence of fibrous cartilage and connective tissue to specific mechanical conditions (Fig. 11).

The characterization of mechanical conditions that determine the tissue differentiation was primarily based on histological studies. Regardless of individual differences in callus formation (Fig. 1b,c and 6a,b) there is still a typical pattern of the tissues involved in bone healing (Fig. 6). Several histological studies have demonstrated that calcification and new bone formation occurs only at existing calcified surfaces (Claes et al., 1955b; Johner, 1972; Johner, 1972; Schenk, 1986; Sevitt, 1981).

We found that intramembranous bone formation was only occurred at low strains and low hydrostatic pressures. These findings are supported by studies performed on stable drill hole defects. Starting at the drill hole surface only intramembranous bone was formed (Claes et al., 1995; Johner, 1972). FEM studies based on these models showed very low strains (maximum 0.08%) and hydrostatic pressure (maximum $-1.3$ kPa) in the drill hole defect (Heigele and Claes, 1997).

For an intramembranous bone formation by osteoid apposition from osteoblasts, a mechanical environment is required that promotes osteoblast activity and proliferation. Our hypothesis of 5% surface strain as a critical strain amplitude for intramembranous bone formation seems to be in accordance with in vitro studies on osteoblasts. Cell culture osteoblasts tried to avoid surface strains larger than 4% by turning away from the principal strain axis (Neidlinger-Wilke et al., 1994).

While high hydrostatic pressures above 0.2 MPa seem to be disadvantageous for bone cells (Ozawa et al., 1990; Seidl et al., 1997), these pressures are not detrimental for chondrocytes. In an epiphyseal growth plate, i.e. endochondral ossification occurs under pressures of about 0.25–1.0 MPa (estimated by loading and cross-sectional area of a growth plate of a young sheep). Therefore, a compressive hydrostatic pressure of about 0.15 MPa might be the critical value that guides the cell differentiation either to an osteoblast or a chondrocyte, or that directs the tissue differentiation either to an intramembranous or an endochondral ossification.

Fig. 9. Third healing stage: global distribution of strain and hydrostatic pressure fields: (a) strain in $x$-direction (%); (b) strain in $y$-direction (%); (c) hydrostatic pressure (MPa).

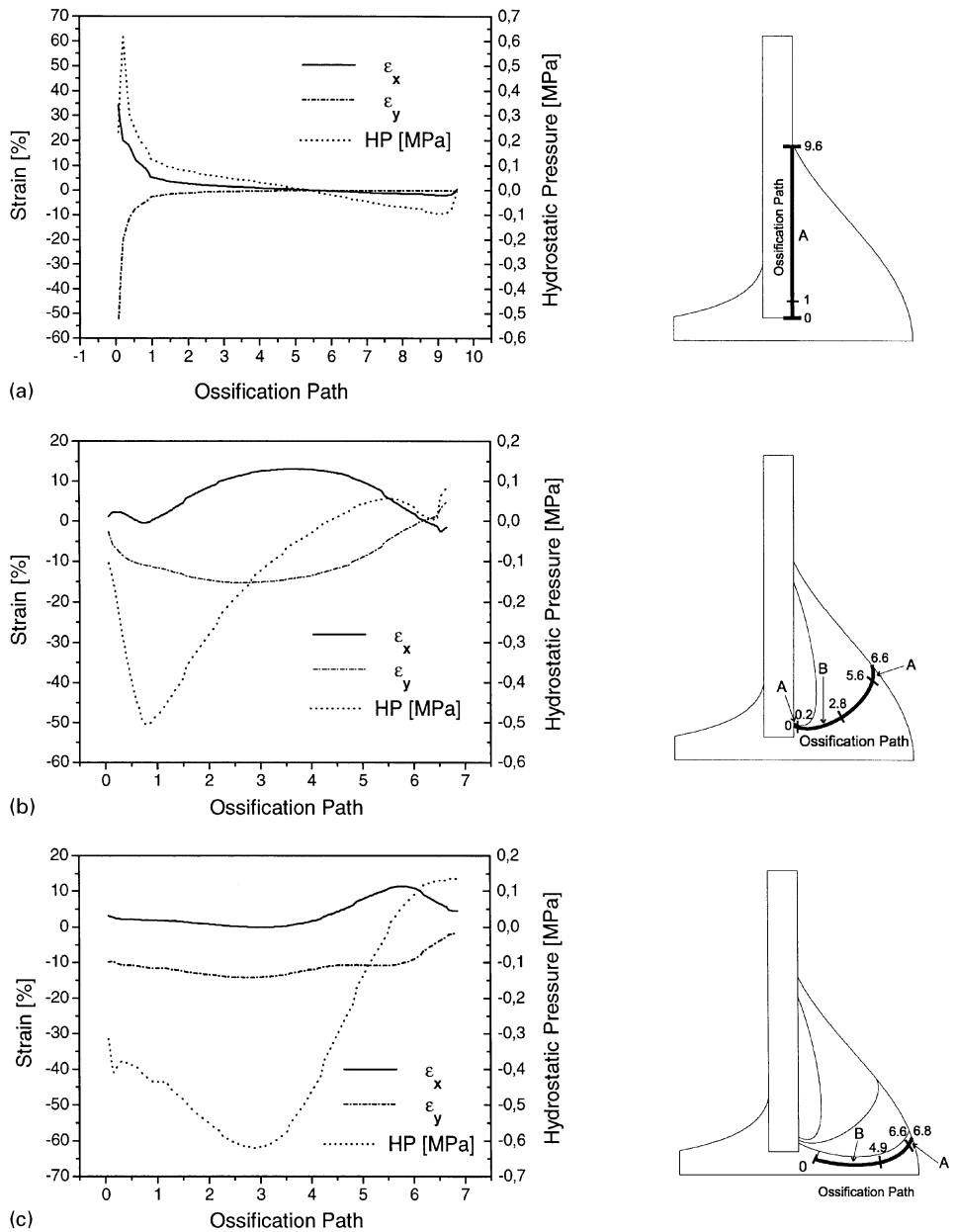


Fig. 10. Calculated strains ($\varepsilon_x$,$\varepsilon_y$) and hydrostatic pressures (HP) along the bony surfaces (ossification paths): (A) surface of intramembranous ossification and $\varepsilon < \pm 5\%$, HP $< \pm 0.15$ MPa; (B) surface of endochondral ossification and $\varepsilon < \pm 15\%$, HP $< -0.15$ MPa. (a) First healing stage (I); (b) second healing stage (II); (c) third healing stage (III).

The characteristic fields of global strain and hydrostatic pressure (Figs. 7–9) showed that in each healing stage the callus tissue exhibits areas with very low and very high mechanical distortions. Therefore we also believe like DiGioia et al. (1986) and Cheal et al. (1991) that it is not adequate to use only the interfragmentary strain (Perren and Cordey, 1980) for describing the tissue response in the fracture callus region.

Our results regarding the global strain and hydrostatic pressure fields (Figs. 7–9) correlate well with the principal results of Carter et al. and Beaupre et al. (Beaupre et al., 1992; Carter et al., 1988). For the loading conditions chosen by Carter et al. (1988) for the first healing stage we calculated similar results. However, in contrast to their work our theory is based on the assumption that new bone formation only occurs on existing bony surfaces and under defined ranges of strain and hydrostatic pressure. Furthermore they have not analysed the mechanical situation quantitatively in terms of strain and pressure.

An investigation based on a finite element model generally has some limitations. The quality of a finite element analysis strongly depends on important parameters

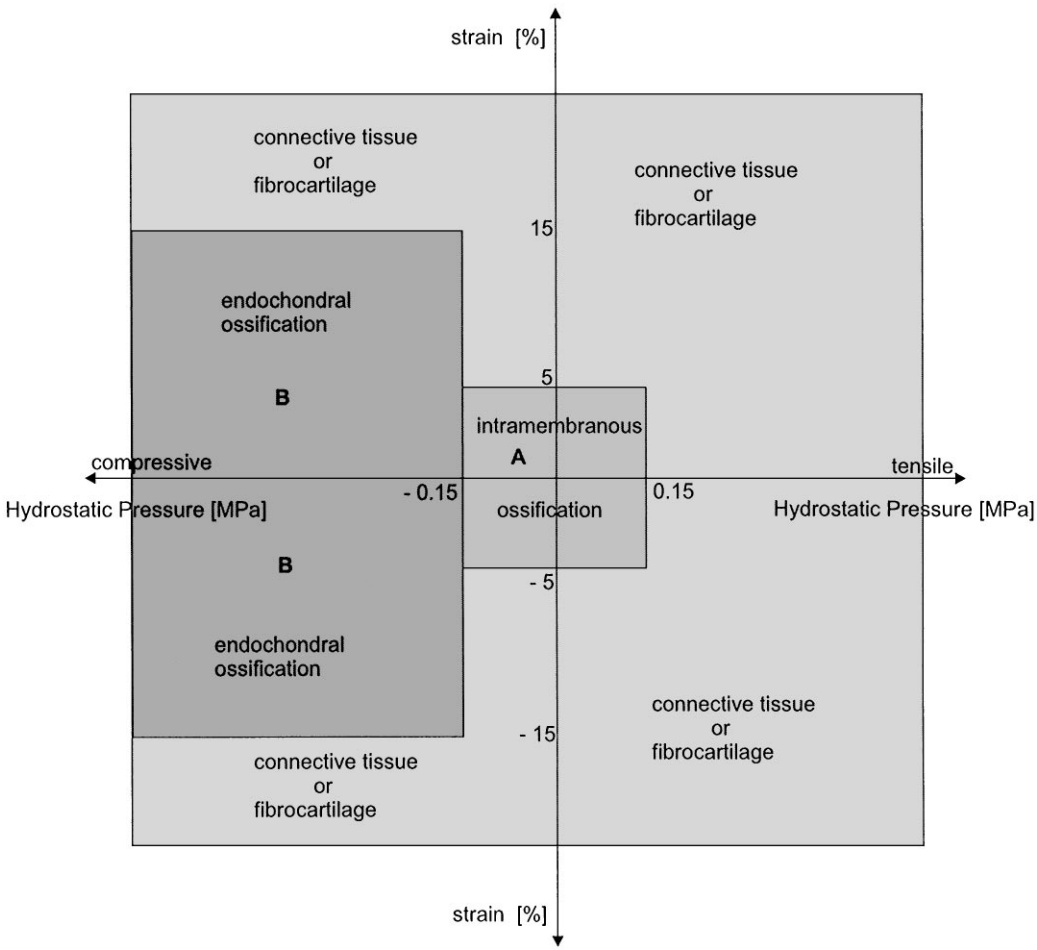


Fig. 11. Hypothesis-based correlations between mechanical conditions and types of tissues in a fracture callus.

such as geometry, material properties or loading conditions (Huiskes and Hollister, 1993). The geometry of the cortex and the callus was grossly idealized. We believe that the presented callus geometry and its mechanical properties are a representative approximation for simple oblique diaphyseal fractures. To our knowledge this was the first attempt to give quantitative boundaries for the differentiation of specific tissue types. We are aware that the limits may vary in a definite region and depend on the applied loads and the specific material properties.

We have presented a quantitative tissue differentiation theory, which correlates new tissue formation with the local mechanical stimuli. The local strains and the hydrostatic pressures within the different types of tissue appeared to be consistent with histological results and knowledge of mechanical effect on cells. The better understanding of the healing process may help us to explain the reasons for different types of fracture healing, for delay of healing, or nonunion. Likewise there is a possibility to improve and optimize internal fixation techniques. To test the generality of this new tissue differentiation theory further finite element studies are required. The present study describes only three separate healing stages. In future studies a progressive healing process can be stimulated by iteratively changing the element material properties.

## Acknowledgements

The study was supported in part by the Deutsche Forschungs Gesellschaft (DFG CL 77/2-1).

## References

Ament, C., Hofer, E.P., Augat, P., Claes, L., 1994. Modeling of tissue transformation processes in fracture healing. Book of Abstracts, 4th Conference of the ISFR, p. 94.

ANSYS User's Manual, vol. III, Elements.

ANSYS User's Manual, vol. IV, Theory.

Ashhurst, D.E., 1986. The influence of mechanical conditions on the healing of experimental fractures in the rabbit: a microscopical study. Philosophical Transactions of the Royal Society of London. 313, 271–302.

Augat, P., Claes, L., 1997. Quantitative assessment of experimental fracture repair by peripheral computed tomography. Calcified Tissue International 60, 194–199.

Augat, P., Claes, L., Simon, J., Suger, G., Fleischmann, W., 1994b. Importance of quality of fracture callus for bone healing. Book of Abstracts. 4th Conference of the ISFR, p. 25.

Augat, P., Margevicius, K., Merk, J., Claes, L., Suger, G., 1994a. Effects of interfragmentary movement and fracture gap size on fracture callus differentiation. Book of Abstracts, 4th Conference of the ISFR, p. 13.

Beaupre, G.S., Giori, N.J., Blenman-Fyhrie, P.R., Carter, D.R., 1992. Modeling fracture healing. The influence of mechanical loading on tissue differentiation. Book of Abstracts, 4th Conference of the ISFR pp. 1–11.

Biegler, F.B., Hart, R.T., 1992. Finite element modeling of long bone fracture healing. In: Middleton, J., Pande, G.N., Williams, K.R. (Eds.), Recent Advances in Computer Methods in Biomechanics and Biomedical Engineering. Books & Journals International LTD, pp. 30–39.

Blenman, P.R., Carter, D.R., Beaupre, G.S., 1989. Role of mechanical loading in the progressive ossification of a fracture callus. Journal of Orthopaedic Research 7, 398–407.

Brand, R.A., Rubin, C.T., 1987. Fracture healing. In: Albrigth, J.A., Brand, R.A. (Eds.), The Scientific Basis of Orthopaedics. Appleton & Lange, Norwalk/Conneticut, pp. 325–340.

Brighton, C.T., 1984. The biology of fracture repair. In: Murray, J.A., (Ed.), Instructional Course Lecturers. C.V. Mosby Co., St. Louis. pp. 60–82.

Carter, D.R., Blenman, P.R., Beaupre, G.S., 1988. Correlations between mechanical stress history and tissue differentiation in initial fracture healing. Journal of Orthopaedic Research 6, 736–748.

Cheal, E.J., Mansmann, K.A., DiGioia, A.M., Hayes, W.C., Perren, S.M., 1991. Role of interfragmentary strain in fracture healing: ovine model of a healing osteotomy. Journal of Orthopaedic Research 9, 131–142.

Claes, L., Augat, P., Wilke, H.-J., Suger, G., Fleischmann, W., Margevicius, K., 1994. The Influence of Interfragmentary Movement on Bone Healing. Book of Abstracts. 4th Conference of the ISFR, p. 24.

Claes, L., Wilke, H.-J., Augat, P., Rübenacker, S., Margevicius, K., 1995a. Effect of dynamization of gap healing of diaphyseal fractures under external fixation. Clinical Biomechanics 8, 227–234.

Claes, L., Wilke, H.-J., Kiefer, H., 1995b. Osteonal structure better predicts tensile strength of healing bone than volume fraction. Journal of Biomechanics 28, 1377–1390.

Davy, D.T., Connolly, J.F., 1982. The biomechanical behaviour of healing canine radii and ribs. Journal of Biomechanics 15, 235–247.

DiGioia, A.M.I., Cheal, E.J., Hayes, W.C., 1986. Threee-dimensional strain fields in a uniform osteotomy gap. Journal of Biomechanical Engineering 108, 273–280.

Duda, G.N., Eckert-Hübner, K., Sokiranski, R., Kreutner, A., Miller, R., Claes, L.E., 1998. Analysis of inter-fragmentary movement as a function of musculoskeletal loading conditions in sheep. Journal of Biomechanics 31, 201–210.

Einhorn, T.A., 1993. Knochenumbau bei der Frakturheilung. Sandorama 2, 15–23.

Einhorn, T.A., 1995. Current concept review enhancement of fracture healing. Journal of Bone and Joint Surgery 77-A(6), 940–956.

Frost, H.M., 1989. The biology of fracture healing. An overview for clinicians. Part I. Clinical Orthopaedics and Related Research 248, 283–293.

Goodship, A.E., Kenwright, J., 1985. The influence of induced micromovement upon the healing of experimental tibial fractures. Journal of Bone and Joint Surgery (Br) 67, 650–655.

Heigele, C., Claes, L., 1997. Finite Elemente Analysen zur Frakturheilung. In: Finite Elemente Workshop 1997. University of Ulm, ISBN: 3-9806183-0-7.

Huiskes, R., Hollister, S.J., 1993. From structure to process, from organ to cell: recent developments of FE-Analysis in orthopaedic biomechanics. Journal of Biomedical Engineering 115, 520–527.

Hulth, A., 1989. Current concepts of fracture healing. Clinical Orthopaedics and Related Research 249, 265–284.

Johner, R., 1972. Zur Knochenheilung in Abhängigkeit von der Defektgröße. Helv Chir Acta. 39, 409–411.

Kenwright, J., Goodship, A.E., 1989. Controlled mechanical stimulation in the treatment of tibial fractures. Clinical Orthopaedics 241, 36–47.

Kenwright, J., Richardson, J.B., Goodship, A.E., Evans, M., Kelly, D.J., Spriggins, A.J., Newman, J.H., Burrough, S.J., Harris, J.D., Rowley, D.I., 1986. Effect of controlled axial micromovement on healing of tibial fractures. Lancet. 2, 1185–1187.

McKibbin, B., 1978. The biology of fracture healing in long bones. Journal of Bone and Joint Surgery (Br) 60, 150–162.

Neidlinger-Wilke, C., Holbein, O., Grood, E., Mörike, M., Claes, L., 1994. Effects of cyclic strain on proliferation, metabolic activity and alignment of human osteoblasts and fibroblasts. Abstract Book, 40th Annual Meeting, ORS, p. 101.

Ozawa, H., Imamura, K., Abe, E., Takahashi, N., Hiraide, T., Shibasaki, Y., Fukuhara, T., Suda, T., 1990. Effect of a continously applied compressive pressure on mouse osteoblast-like cells (MC3T3-E1) in vitro. Journal of Cell Physiology 142, 177–185.

Pauwels, F., 1960. Eine neue Theorie über den Einfluß mechanischer Reize auf die Differenzierung der Stützgewebe. Z Anat Entwicklungsgeschichte 121, 478–515.

Perren, S.M., 1974. Biomechanik der Frakturheilung. Orthopäde 3, 135–139.

Perren, S.M., Cordey, J., 1980. The concept of interfragmentary strain. In: Uhthoff, H.K., (Ed.), Current Concepts of Internal Fixation of Fractures, Springer, Berlin, pp. 63–77.

Rhinelander, F.W., 1979. Vascular proliferation and blood supply during fracture healing. In: Brooker, A.F., Edwards, C.C., (Eds.), External Fixation: The Current State of the Art. The Williams and Wilkins Co, Baltimore, pp. 9–14.

Schenk, R.K., 1986. Histophysiology of bone remodelling and bone repair. In: Lin, O.C., Chao, E.Y.S., (Eds.), Perspectives on Biomaterials. Elsevier Science, Amsterdam, pp. 75–94.

Seidl, W., Kaspar, D., Neidlinger-Wilke, C., Claes, L., 1997. Influence of cyclic strain amplitude on proliferation of a human osteoblast-like cell line. Book of Abstracts. 25th European Symposium on Calcified Tissues. Harrogate, p. 354.

Sevitt, S., 1981. Secondary repair of fractures. Events preparatory to union. In: Sevitt, S., (Ed.), Bone Healing and Fracture Repair in Man. Churchill Livingstone.

Simmons, D.J., 1985. Fracture healing perspectives. Clinical Orthopaedics and Related Research 200, 100–113.

Sussman, T., Bathe, K.J., 1987. A finite element formulation for nonlinear incompressible elastic and inelastic analysis. Computers and Structures 26, 357–409.

Willenegger, H., Perren, S.M., Schenk, R., 1971. Primäre und sekundäre Knochenheilung. Chirurgia 42, 241–252.